Exposing Multiple Roles of H_2O in High-Temperature Enhanced Carbon Nanotube Synthesis

M. Bystrzejewski,[†,‡] R. Schönfelder,[†] G. Cuniberti,[§] H. Lange,[‡] A. Huczko,[‡] T. Gemming,[†] T. Pichler,[||] B. Büchner,[†] and M. Rümmeli*[,†]

IFW Dresden, P.O. Box 270116, D-01171 Dresden, Germany, Department of Chemistry, Warsaw University, 02-093 Warsaw, Poland, Institute for Materials Science and Max Bergmann Center of Biomaterials, Dresden University of Technology, D-01062 Dresden, Germany, and Department of Physics, Vienna University, A-1090 Vienna, Austria

Received July 29, 2008
Revised Manuscript Received September 27, 2008

The synthesis of single-wall carbon nanotubes (SWNTs), regardless of synthesis route, also generates significant amounts of undesired impurities such as catalyst particles, amorphous carbon, and graphitic particles. The need for pure samples is important and for certain applications or studies is paramount. A variety of postsynthesis purification procedures have been developed to remove impurities. Usually, a combination of purification steps are employed, most of which exploit oxidation. A disadvantage is that many lead to the partial etching of SWNTs and damage their structure. Less-aggressive oxidizing agents have also been explored. The use of steam can efficiently etch amorphous carbon and open the ends of single and multiwalled carbon nanotubes.[1] CO_2 is another weak oxidizer that can selectively remove amorphous carbon.[2] Obviously, the direct synthesis of high purity SWNTs is far more attractive. A well-known example is the synthesis route developed by Hata et al.[3] They demonstrated that small additions of water vapor (50−290 ppm) to the buffer gas during the chemical vapor deposition (CVD) of supported catalysts yields superdense and vertically aligned ultralong SWNTs. They claim this technique leads to SWNTs purities above 99%. This type of approach can eliminate the need for postsynthesis processing. However, SWNTs fabricated via CVD tend to possess higher structural disorder, large diameter distributions and usually include a fraction of multiwalled carbon nanotubes (MWNTs) as compared to floating catalyst techniques such as the high-pressure carbon monoxide (HiPCO) process or laser evaporation.[4] Remarkably, though, we have found no reports on the use of water vapor in laser ablation reactions for the formation of SWNTs. The potential advantages of high-purity SWNT samples with few defects and a narrow diameter distribution are obvious.

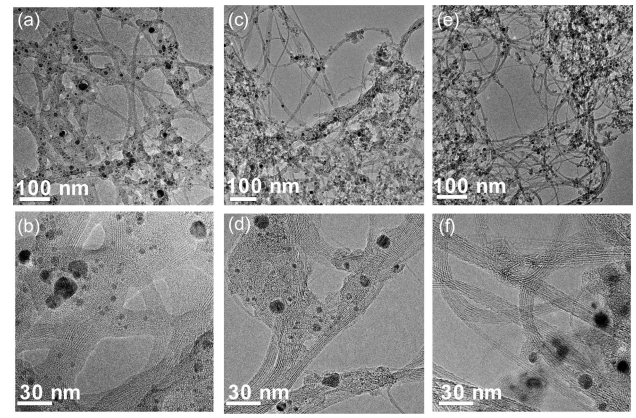

Figure 1. TEM micrographs of as-produced SWNTs from laser evaporation with different H_2O content: (a, b) 3, (c, d) 135, and (e, f) 1227 ppm.

In this work, we investigate the influence of water vapor on the formation of SWNTs in laser ablation. The SWNTs were synthesized using a furnace-based laser ablation process discussed elsewhere.[4,5] In brief, the evaporation of the target was driven by a Nd:YAG laser (ca. 2 GW per pulse at 10 Hz). The ternary catalyst was composed from nickel, cobalt, and molybdenum (5:4:1 respectively). The oven temperature was maintained at 1200 °C in each test.

All experiments were performed in a N_2 atmosphere at a pressure of 101 kPa and a gas flow rate of 0.4 slpm. The water vapor was controlled via mass flow controllers from 3 to 2063 ppm (commercial dry N_2 has a water vapor content of 3 ppm). N_2 saturated with water vapor was achieved by bubbling the N_2 through a stainless steel scrubber (22 °C). Typical ablation times were 120 s. The products were collected on a water-cooled copper finger behind the target. The average mass reduction of the target was 20 mg, which corresponds to an erosion rate rate of 10 mg/min. No differences in the erosion rate were observed when including H_2O. The optical absorption spectroscopic (OAS) studies were conducted on a Bruker IFS 113V. A Bruker IFS100 spectrometer (1064 nm) was used for the Raman measurements. For transmission electron microscopy (TEM) investigations (FEI Tecnai F30), the samples were directly pressed on standard Cu TEM grids.

Detailed TEM studies for all samples showed the samples to comprise SWNTs bundles, catalyst particles, and amorphous carbon. The amount of amorphous carbon was seen to decrease with increasing water content. In Figure 1, TEM images for 3 samples (3, 135, and 1227 ppm) show the

* Corresponding author. E-mail: m.ruemmeli@ifw-dresden.de.
† IFW Dresden.
‡ Warsaw University.
§ Dresden University of Technology.
|| Vienna University.

(1) Chiang, I. W.; Brinson, B. E.; Huang, A. Y.; Willis, P. A; Bronikowski, M. J.; Margrave, J. L.; Smalley, R. E.; Hauge, R. H. *J. Phys. Chem. B* **2001**, *106*, 8297.
(2) Magrez, A.; Seo, J. W.; Kuznetsov, V. L.; Forro, L. *Angew. Chem., Int. Ed.* **2007**, *46*, 441.
(3) Hata, K.; Futaba, D. N.; Mizuno, K.; Namai, T.; Yumura, M.; Iijima, S. *Science* **2004**, *306*, 1362.
(4) Rummeli, M. H.; Kramberger, C.; Loffler, M.; Jost, O.; Bystrzejewski, M.; Gruneis, A.; Gemming, T.; Pompe, W.; Buchner, B.; Pichler, T. *J. Phys. Chem. B* **2007**, *111*, 8234.
(5) Rummeli, M. H.; Borowiak-Palen, E.; Gemming, T.; Pichler, T.; Knupfer, M.; Kalbac, M.; Dunsch, L.; Jost, O.; Silva, S. R. P.; Pompe, W.; Buchner, B. *Nano Lett.* **2005**, *5*, 1209.

10.1021/cm8020676 CCC: $40.75
Published on Web 10/22/2008

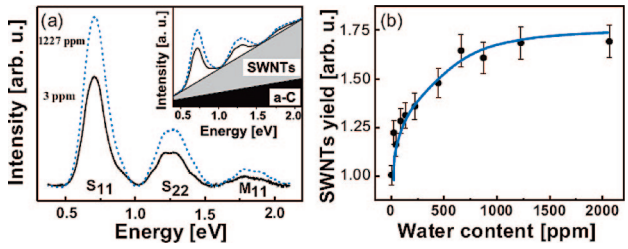

Figure 2. (A) Normalized and strapped electronic spectra from SWNTs; black curve, 3 ppm H_2O; blue curve, 1227 ppm H_2O. Inset: Normalized electronic spectra sitting on π plasmon tail. (B) SWNT yield versus H_2O content in laser evaporation reaction (curve is to guide the eye).

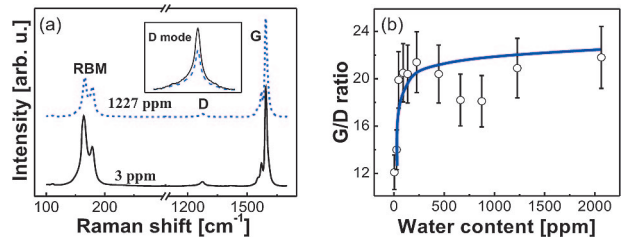

Figure 3. (A) Raman spectra from SWNTs; black curve, 3 ppm H_2O; blue curve, 1227 ppm H_2O. Inset: Expanded D modes after normalization to G mode. (B) G/D ratio versus H_2O content in laser evaporation reaction (curve is to guide the eye).

reduction in amorphous material as the water content is increased. Although the data suggest that the presence of water in the laser ablation reaction reduces amorphous C species, caution should be exercised as TEM studies monitor only picogram quantities of the samples. Hence, we conducted additional studies. The absorption spectra of SWNTs typically contain 3 prominent peaks from interband transitions. The first and most intense pair, from semiconducting tubes, are termed the S_{11} and S_{22} transitions. The third, M_{11}, stems from metallic SWNTs. The peak widths correspond to the sample diameter distribution and can be used to determine the mean diameter. We did not observe any shift in any of the peaks with increasing water content (Figure 2a). The mean diameter as determined from the most prominent peak, S_{11}, was 1.26 nm $\pm$ 0.01 nm after correction for exciton effects.[5] The interband peaks sit on a background originating from the π plasmon from carbon species, namely, SWNTs and carbonaceous impurities (Figure 2a, inset). Hence, comparison of the SWNT interband peaks with the background provides a measure of the purity.[6] Figure 2a highlights the relative increase in yield for two water contents, 3 and 1227 ppm.

Figure 2b shows the quantitative changes in purity (SWNTs relative to amorphous carbon) determined from the areas of the S_{11} peak after normalization and strapping the background. The data show a nonlinear behavior; the relative SWNTs yield increase decays with increasing water content so that by 700 ppm the improved yield is stable. Changes are also observed in the Raman spectroscopic data. The presence of the radial breathing modes in the spectra verifies that the structures are SWNTs (Figure 3a). The diameters in

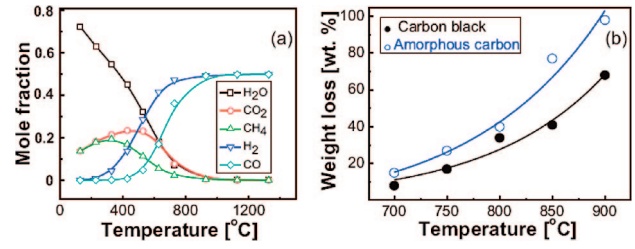

Figure 4. (A) Calculated equilibrium compositions from water and carbon at various temperatures. (B) Weight loss versus temperature (in steam) for amorphous carbon and carbon black (curves are to guide the eye).

resonance for these samples using the expression[7] $\omega = 223/d_t + 10$ correspond to diameters between 1.18 and 1.27 nm, in good agreement with the OAS data. At higher frequencies the D (disorder) mode and G (graphitic) modes are observed. The G peaks (1565−1595 cm^{-1}) arise from (tangential) C−C stretching in the graphene plane and in these samples they are clearly separated, which is also a characteristic of SWNTs. Often, the quality of SWNTs is defined as a measure of the G/D ratio, because it is argued that the intensity of the D mode is activated by defects in the tubes.[8] In these trials, the G/D ratio is seen to rapidly improve with small increases in water vapor, after which little further improvement is obtained (at ca. 50 ppm). This improved crystallinity shows that the role of water is more than simply the removal of amorphous carbon. The improved G/D ratio (almost 100%), even with very small amounts of H_2O, does not occur in tandem with the reduction of amorphous carbon as shown in the OAS data. Hence, although a reduction in amorphous species might contribute to a reduced D mode, the observed difference between the Raman and OAS data highlights a previously undisclosed role for H_2O enhanced SWNTs synthesis.

Both the electron microscopy and OAS studies show the inclusion of water reduces the amorphous carbon content in the as produced sample. This is in agreement with Hata's supergrowth work (550−750 °C), which points to water induced oxidation of amorphous carbon.[4] In our studies, not only is the background temperature higher, 1200 °C, but so is that of the laser generated evaporation plume, which exceeds 3000 °C. Thus, we can expect H_2O in the presence of C to evolve into other species during the reaction. As a first approximation to better understand the role of water with carbon at elevated temperatures, we conducted thermodynamic calculations (FactSage Equilib-Web Package). The calculated equilibrium compositions are presented in Figure 4a. The results show that under equilibrium conditions at typical CVD temperatures (550−750 °C), one might expect CO_2, CH_4, H_2, and CO to be present. At 1200 °C, we can expect the presence of CO and H_2. However, although these species might form because of oven heating, the nonequilibrium plume temperatures are sufficient to atomize H_2 and CO, providing a source of H and O. The roles of O and H was explored by Dai and co-workers using oxygen-assisted

(6) Itkis, M. E.; Perea, D.; Jung, R.; Niyogi, S.; Haddon, R. C. *J. Am. Chem. Soc.* **2004**, *127*, 3439.
(7) Fantini, C.; Jorio, A.; Souza, M.; Dresselhaus, M. S.; Pimenta, M. A. *Phys. Rev. Lett.* **2004**, *93*, 147406.
(8) Dillon, A. C.; Parilla, P. A.; Alleman, J. L.; Gennett, T.; Jones, K. M.; Heben, M. J. *Chem. Phys. Lett.* **2004**, *401*, 522.

hydrocarbon CVD.[9] They point out that hydrogen species are unfavorable to SWNTs formation because H radicals etch the SWNTs. They argue that if oxygen is available, it can remove hydrogen by OH formation. Alcohol CVD studies by Maruyama et al. point to OH removing amorphous carbon species.[10] Further, H_2O can also etch amorphous carbon preferentially over SWNTs. This is highlighted in Figure 4b, which shows the weight loss of amorphous carbon and carbon black for different temperatures in steam. It is obvious that the weight loss for carbon black, which has more ordered carbon, is less than for the amorphous carbon. One can anticipate highly crystalline SWNTs to be significantly less sensitive to H_2O etching. The preferential etching of disordered carbon is then a trait of H_2O and OH but not hydrogen.

Despite the cleansing efficiency of H_2O (and OH), we still obtain some amorphous carbon species as highlighted by the TEM studies. We attribute this to the short residence time of species in the reaction zone limiting the efficiency of the process.

We now turn to the Raman spectroscopic data that show a dramatic increase in the G/D ratio for only small quantities of water (up to 50 ppm), after which little further improvement is obtained. The enhanced crystallinity suggests an improved growth process in the reaction. Previous studies of ours in which the role of oxygen[5] and hygrogen[11] were explored in laser evaporation show that both oxygen and hydrogen can activate catalysts, viz. they promote nanotube growth. The role of H in this presented study is probably weak, because H can etch the SWNTs themselves and so increase the D mode. This is contrary to our observations and points to oxygen activating the catalysts. Various other studies also indicate an oxygen role in catalyst activation. For example, CVD studies have shown oxygen-based activation of both metallic and nonmetallic catalysts,[12,13] XPS studies on CNT grown from SiC show O chemically bound to C,[14] catalyst free growth of CNT can be obtained in oxy-fuel flames,[15] and oxygen from oxides can also be involved with CNT growth.[16,17] Importantly, studies with oxygen-containing gases show oxygen accelerates graphitization.[18] We postulate that oxygen (and possibly hydrogen) plays a role in the growth of the CNT by promoting the graphitisation of carbon at the root of a growing tube.

In summary, our results indicate that the inclusion of water in the synthesis of SWNTs not only plays a cleansing role by removing amorphous carbon species but also plays an additional indirect role in growth promotion. The high temperatures achieved in the laser evaporation plume enable the formation of atomic oxygen and hydrogen. The reactive nature of these species likely accounts for the improved crsytallinity of the water enhanced SWNTs, perhaps playing a role at the root of a growing tube. This points to oxygen and hydrogen as growth promoters.

Acknowledgment. M.B. acknowledges support from the DFG RU1540/1−1 and the SMWK. M.H.R thanks the DFG PI440/4. H.L. thanks the N204 096 31/2160. We are grateful to R. Hübels and S. Leger for technical support.

CM8020676

(9) Zhang, G.; Mann, D.; Zhang, L.; Javey, A.; Li, Y.; Yenilmez, E.; Wang, Q.; McVittie, J. P.; Nishi, Y.; Gibbons, J.; Dai, H. *Proc. Natl. Acad. Sci., U.S.A.* **2005**, *102*, 16141.
(10) Maruyama, S.; Kojima, R.; Miyauchi, Y.; Chiashi, S.; Kohno, M. *Chem. Phys. Lett.* **2002**, *360*, 229.
(11) Bystrzejewski, M.; Rummeli, M. H.; Lange, H.; Huczko, A.; Baranowski, P.; Gemming, T.; Pichler, T. *J. Nanosci. Nanotechnol.* **2008**, in press.
(12) Takagi, D.; Homma, Y.; Hibino, H.; Suzuki, S.; Kobayashi, Y. *Nano Lett.* **2006**, *6*, 2642.
(13) Takagi, D.; Hibino, H.; Suzuki, S.; Kobayashi, Y.; Homma, Y. *Nano Lett.* **2007**, *7*, 2272.
(14) Lu, W.; Boeckl, J.; Mitchel, W. C.; Rigueur, J. l.; Collins, W. E. *Mater. Sci. Forum* **2006**, *1575*, 527.
(15) Merchan-Merchan, W.; Savaliev, A.; Kennedy, L. A.; Fridman, A. *Chem. Phys. Lett.* **2002**, *354*, 20.
(16) Rummeli, M. H.; Kramberger, C.; Gruneis, A.; Ayala, P.; Gemming, T.; Buchner, B.; Pichler, T. *Chem. Mater.* **2007**, *19*, 4105.
(17) Rummeli, M. H.; Schaffel, F.; Kramberger, C.; Gemming, T.; Bachmatiuk, A.; Kalenczuk, R. J.; Rellinghaus, B.; Buchner, B.; Pichler, T. *J. Am. Chem. Soc.* **2007**, *129*, 15772.
(18) Noda, T.; Inagaki, M. *Carbon* **1964**, *2*, 127.